RECENT DEVELOPMENTS IN EARTH OBLATENESS MODELING FOR ATTITUDE DETERMINATION*

M. Challa
(mchalla@csc.com)
Applied Research Department
Computer Sciences Corporation
10110 Aerospace Road
Lanham-Seabrook (MD 20706) USA

G. Natanson
(gnatanso@csc.com)
Mission System Engineering Department
Computer Sciences Corporation
7700 Hubble Drive
Lanham-Seabrook (MD 20706) USA

Abstract

The horizon contour presented to a spacecraft observing an oblate Earth is analyzed by relating the angular radius of the horizon from the nadir vector to the azimuthal angle about this vector. It is shown that the horizon contour is an ellipse with respect to the geocentric nadir vector, and exact formulas are derived for various properties of the horizon ellipse. Similar analysis, linearized in an Earth oblateness parameter, is presented for the geodetic nadir vector and, for applications in static horizon sensors, the horizon bisector nadir. Numerical calculations for the Tropical Rainfall Measuring Mission (TRMM) are used to show that the geodetic and the horizon bisector nadir vectors are nearly perpendicular to the horizon ellipse, and that approximating the horizon contour as a circle about the geodetic nadir introduces errors of less than 0.06 degrees.

***Key words**:* Earth oblateness, horizon ellipse, geocentric nadir, geodetic nadir, horizon bisector nadir, TRMM

Introduction

Low Earth orbiting spacecraft commonly use sensors that sense the Earth infrared horizon to compute the attitude. An important task is to know the shape of the Earth disk as observed by the spacecraft, for then we can compute the reference vector (the nominal pointing direction), and compare with the sensor observations to obtain the attitude (e. g., roll and pitch). For accurate attitude determination, we must take into account that the Earth must be modeled not as a sphere but as an oblate ellipsoid[1]. If a (≈ 6378.140 km) and b (≈ 6356.755 km) are respectively the equatorial and polar radii of the Earth, a flattening factor, α, can be defined as

$$\alpha = \frac{a^2}{b^2} - 1 \ . \tag{1}$$

(Note that α is small, only 0.006740 or about 1/150, a fact which will be useful in generating formulas linearized in α later.) The Earth ellipsoid may then be written as

$$x^2 + y^2 + (1+\alpha)z^2 = a^2 \tag{2}$$

where (x, y, z) are the geocentric inertial (GCI) frame coordinates of any point $\vec{r}$ on the surface.

For attitude determination purposes, the crucial question may be phrased as (see Figure 1 below): how does the angular distance, ρ, of the horizon from the nadir vary as a function of the azimuthal angle, ψ? (Note that Fig. 1 gives only a general sketch of these quantities; a precise definition of the plane of the figure depends on the definition of the spacecraft nadir vector, and will be offered in subsequent sections.)

The Earth oblateness complicates the issue in two ways as will be shown below. First, the horizon points do not lie on a circle; rather, they lie on an ellipse. Second, we must be careful in specifying what we mean by the spacecraft nadir direction. Let the spacecraft be at $\vec{R}$ with respect to the geocenter, with GCI coordinates (X, Y, Z) and $R = |\vec{R}|$. Denoting unit vectors by "^", we

* This work was supported by NASA/GSFC, Greenbelt, MD, under Contract GS -35F-4381G, Task Order No. S-24280-G.

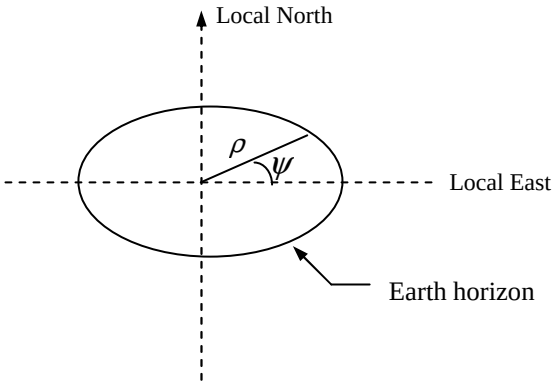

Figure 1. Sketch of the Earth Disk Apparent to a Spacecraft Showing the Angular Radius from the Nadir, ρ, and the Azimuthal Angle ψ

shall refer hereafter to three different nadir vectors - the geocentric ($\hat{n}_C$), the geodetic ($\hat{n}_D$), and the horizon bisector ($\hat{n}_H$) - which are defined as follows. $\hat{n}_C \equiv -\vec{R}/R$, $\hat{n}_D$ is the direction of the perpendicular from the spacecraft to the Earth's surface, and $\hat{n}_H$ is the unit vector in the direction which equalizes the values of ρ for the local North and South horizon points.

Let (ρ_C, ψ_C), (ρ_D, ψ_D), and (ρ_H, ψ_H), denote ρ and ψ when the nadir is $\hat{n}_C$, $\hat{n}_D$, and $\hat{n}_H$ respectively. The question posed earlier may now be restated as: what are the functional relationships $\rho_C(\psi_C)$, $\rho_D(\psi_D)$, and $\rho_H(\psi_H)$? The problem was partly solved in Ref. 1 where an exact result for $\rho_C(\psi_C)$ was presented. Our principal objectives here are: to fully develop the properties of the horizon ellipse, and to examine the other two angular radii - $\rho_D(\psi_D)$ and $\rho_H(\psi_H)$. Note that $\rho_D(\psi_D)$ is important on account of most Earth-pointing spacecraft being geodetic-pointing (i. e., the spacecraft $\hat{z}$ -axis is nominally aligned with $\hat{n}_D$), and $\rho_H(\psi_H)$ being necessitated by newer static Earth sensors[2,3] where nominal pointing implies equal values of ρ in diametrically opposite horizon quadrants.

The material presented here is mainly derived from References 1-7, and consists of the following principal results.

- The locus of the horizon points seen by the spacecraft is an ellipse whose plane is *not* perpendicular to $\hat{n}_C$.
- An exact formula relating ρ_C to ψ_C.
- Approximate formulas for computing $\hat{n}_D$ and $\hat{n}_H$.
- $\hat{n}_C$ and $\hat{n}_D$ differ substantially (by nearly 0.2 deg), but $\hat{n}_D$ and $\hat{n}_H$ are approximately the same (to within 0.01 deg).
- $\hat{n}_D$ and $\hat{n}_H$ are both nearly normal to the horizon ellipse (to within 0.02 deg).
- Analytical expressions linearized in α for $\rho_D(\psi_D)$ and $\rho_H(\psi_H)$.
- Approximating $\rho_D(\psi_D)$ by a circle which depends on the spacecraft position introduces errors less than 0.06 deg.

The numerical values quoted are for the Tropical Rainfall Measuring Mission[8] (TRMM) - a typical geodetic-pointing spacecraft of altitude 350 km and inclination 35 degrees (deg).

Additional notation used here is as follows. The GCI frame is defined by the unit vectors $\{\hat{x}_I, \hat{y}_I, \hat{z}_I\}$. $\vec{h}$ is the vector from the spacecraft to a horizon point. ρ_0 is the angular radius of the circular disk presented by a fictitious spherical Earth of radius *a*, i.e.,

$$\sin(\rho_0) = a/R. \tag{3}$$

We use the compact notation "*c(θ) = cos(θ)*", "*s(θ) = sin(θ)*", and "*t(θ) = tan(θ)*". λ and γ are the spacecraft geocentric latitude and right ascension respectively, so that the GCI components of $\vec{R}$ can also be written as $R\big(c(\lambda)c(\gamma), c(\lambda)s(\gamma), s(\lambda)\big)$.

The Horizon Ellipse

As shown by K. Liu[1], the horizon points lie in the *horizon plane*

$$xX + yY + (1+\alpha)zZ = a^2 \tag{4}$$

with (x, y, z) subject to Eq. (2). It is convenient to examine the locus of the horizon points in a new frame $\{\hat{x}', \hat{y}', \hat{z}'\}$ which is obtained by rotating $\{\hat{x}_I, \hat{y}_I, \hat{z}_I\}$ first through $\gamma - \frac{\pi}{2}$ about $\hat{z}_I$, and then through λ about the intermediate *x*-axis so that $\hat{y}'$ coincides with $\vec{R}$. The transformation matrix from $\{\hat{x}_I, \hat{y}_I, \hat{z}_I\}$ to $\{\hat{x}', \hat{y}', \hat{z}'\}$ is:

$$A = \begin{bmatrix} s(\gamma) & -c(\gamma) & 0 \\ c(\lambda)c(\gamma) & c(\lambda)s(\gamma) & s(\lambda) \\ -s(\lambda)c(\gamma) & -s(\lambda)s(\gamma) & c(\lambda) \end{bmatrix}. \tag{5}$$

Labeling the surface points as (x', y', z') in the new frame, Eq. (2) becomes

$$x'^2+\left(1+\alpha\, s^2(\lambda)\right)y'^2+\left(1+\alpha\, c^2(\lambda)\right)z'^2+ 2\alpha\, s(\lambda)\, c(\lambda)\, y'\, z'=a^2\ , \tag{6}$$

and Eq. (4) becomes

$$\left(1+\alpha\, s^2(\lambda)\right)y'+\alpha\, s(\lambda)\, c(\lambda)\, z'=a^2/R\ . \tag{7}$$

Eliminating y' in Eqs. (6) and (7) yields the *horizon ellipse* in the $\hat{x}'$–$\hat{z}'$ plane:

$$x'^2+\left(1+\alpha'\right)z'^2=a'^2\,, \tag{8}$$

where:

$$a'^2=R^2s^2(\rho_0)\left[\frac{1+\alpha\, s^2(\lambda)-s^2(\rho_0)}{1+\alpha\, s^2(\lambda)}\right], \tag{9a}$$

$$b'^2=R^2s^2(\rho_0)\left[\frac{1+\alpha\, s^2(\lambda)-s^2(\rho_0)}{1+\alpha}\right], \tag{9b}$$

and

$$\alpha'=\frac{a'^2}{b'^2}-1=\frac{\alpha\, c^2(\lambda)}{1+\alpha\, s^2(\lambda)}\ . \tag{9c}$$

Note that $\vec{R}$ passes through the center of the ellipse.

An Exact Relation Between ρ_C and ψ_C

In view of its importance, we will now derive Eq. (4-24) of Ref. 1 which was given without proof. Consider Fig. 2 where u is the length of the perpendicular from a horizon point (x', y', z') to $\vec{R}$. We have

$$\cot(\rho_C)=\frac{R-y'}{u}\ . \tag{10}$$

To relate u to ψ_C, note that the $\hat{x}'$ axis is along local West and the $\hat{z}'$ axis is along local North in Fig. 1 so that

$$x'=-u\ c(\psi_C)\ ,\quad z'=u\, s(\psi_C)\ . \tag{11}$$

Using Eq. (11) in Eq. (8), and using the definitions in Eqs. (9), yields

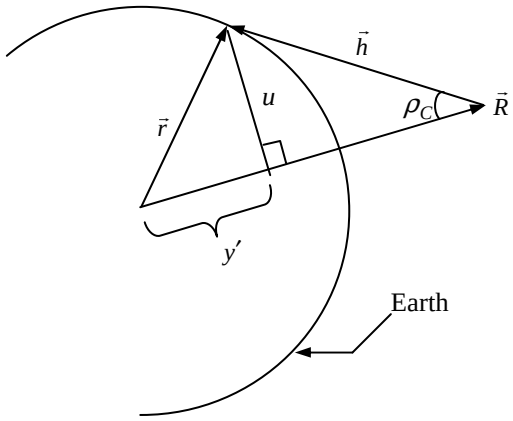

Figure 2. Geometry Used in Relating ρ_C to ψ_C

$$u(\psi_C)=\frac{a\ f_1(\lambda)}{R\ f_2(\lambda,\psi_C)} \tag{12}$$

where

$$f_1(\lambda)=\sqrt{R^2\left(1+\alpha\, s^2(\lambda)\right)-a^2} \tag{13}$$

and

$$f_2(\lambda,\psi_C)=\sqrt{1+\alpha\, s^2(\lambda)+\alpha\, c^2(\lambda)\, s^2(\psi_C)}\ . \tag{14}$$

It remains to obtain $y'(\psi_C)$ in Eq. (10). To do this, eliminate u in Eqs. (11) and (12), and use the resulting $z'(\psi_C)$ in Eq. (7). This yields

$$y'(\psi_C)=\frac{a\left(a\ f_2-\alpha\, s(\lambda)c(\lambda)\, s(\psi_C)\, f_1\right)}{R\left(1+\alpha\, s^2(\lambda)\right)f_2}\ . \tag{15}$$

Using Eqs. (12) and (15) in Eq. (10) yields

$$\cot(\rho_C)=\frac{f_1 f_2+a\,\alpha\, s(\lambda)\, c(\lambda)\, s(\psi_C)}{a\left(1+\alpha\, s^2(\lambda)\right)} \tag{16}$$

which is Eq. (4-24) of Reference 1. (Note that Ref. 1 uses the factor f related to α by

$\alpha = \dfrac{1}{(1-f)^2} - 1$ to express the Earth oblateness.)

The Horizon Ellipse Expressed in a Horizon Plane Frame

Let $\hat{m}$ be the normal to the horizon plane. From Eq. (7), we get

$$\hat{m} = \frac{\left(0, 1+\alpha\, s^2(\lambda), \alpha\, s(\lambda)\, c(\lambda)\right)}{\sqrt{1+\left(2\alpha+\alpha^2\right) s^2(\lambda)}} \ . \qquad (17)$$

If ε_{ell} is the angle between $\hat{m}$ and $\hat{y}'$ (i. e., $\vec{R}$), a direct consequence of the Earth oblateness is that $\varepsilon_{ell} \neq 0$:

$$c(\varepsilon_{ell}) = \frac{1+\alpha\, s^2(\lambda)}{\sqrt{1+\left(2\alpha+\alpha^2\right) s^2(\lambda)}}, \qquad (18)$$

Thus ε_{ell} is a small angle, and it is easy to show that

$$\varepsilon_{ell} \approx \frac{\alpha}{2}\, s(2\lambda) \ . \qquad (19)$$

It is worthwhile to examine the ellipse in the $\{\hat{x}'', \hat{y}'', \hat{z}''\}$ frame which is obtained by further rotating the $\{\hat{x}', \hat{y}', \hat{z}'\}$ frame through the angle ε_{ell} about the $\hat{x}'$ axis so that the ellipse lies in the $\hat{x}''$–$\hat{z}''$ plane. Labeling the horizon points as (x'', y'', z''), Eq. (8) becomes

$$x''^2 + (1+\alpha')\left[\, s(\varepsilon_{ell})\, y'' + c(\varepsilon_{ell})\, z'' \,\right]^2 = a'^2 , \qquad (20)$$

while Eq. (15) shows that y'' is constant on the horizon ellipse:

$$y'' = \frac{a^2}{R\sqrt{1+\left(\alpha^2 + 2\alpha\right) s^2(\lambda)}} \ . \qquad (21)$$

Note that the above value of y'' is also the perpendicular distance from the geocenter to the horizon ellipse. Thus the center of the horizon ellipse is shifted along $\hat{z}''$ through

$$\Delta z'' = \frac{a^2\, \alpha\, s(\lambda)\, c(\lambda)}{R\left(1+s^2(\lambda)\right)\sqrt{1+\left(\alpha^2 + 2\alpha\right) s^2(\lambda)}} \ . \qquad (22)$$

Nadir Coordinate Systems

The scheme used to generate the $\{\hat{x}'', \hat{y}'', \hat{z}''\}$ frame from the $\{\hat{x}', \hat{y}', \hat{z}'\}$ frame can be generalized to yield a family of spacecraft-centered frames which we term "Nadir Coordinate Systems" (NCSs) and denote by $\{\hat{x}_N, \hat{y}_N, \hat{z}_N\}$. The essential aspect of a NCS is that it is generated from the $\{\hat{x}', \hat{y}', \hat{z}'\}$ frame by a rotation about the $\hat{x}'$ axis through an angle ε_N (see Figure 3). This allows us to adopt a common treatment for analyzing $\rho_D(\psi_D)$ and $\rho_H(\psi_H)$ by introducing the tilt angles ε_D and ε_H.

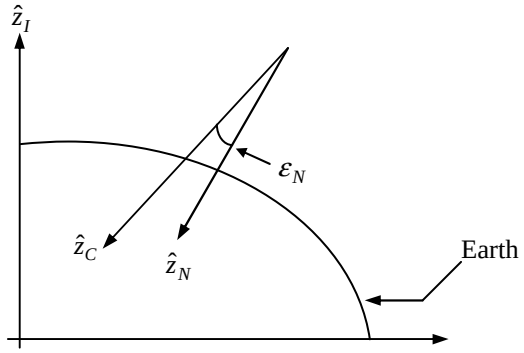

Fig 3. Generation of a Nadir Coordinate System by Tilting the Geocentric Nadir Through ε_N

Analogous to conventional definitions of orbital coordinate systems, the NCS axes are defined as follows.

$\hat{x}_N$ (local East) = - $\hat{x}'$
$\hat{z}_N$ = nadir direction, $\hat{n}_N$, obtained by tilting - $\hat{y}'$ through an angle ε_N about $\hat{x}'$
$\hat{y}_N$ (local South) = $\hat{z}_N \times \hat{x}_N$

The angle ψ_N is measured from local East, as in Fig. 1. In particular, the Geocentric NCS, $\{\hat{x}_C, \hat{y}_C, \hat{z}_C\}$, is defined by $\varepsilon = 0$, i.e., by relabeling the $\{\hat{x}', \hat{y}', \hat{z}'\}$ axes:

$$\hat{x}_C = -\hat{x}' , \ \hat{y}_C = -\hat{z}' , \ \hat{z}_C = -\hat{y}' . \qquad (23)$$

It is easy to see that the nadir vector, $\hat{z}_N$, can be resolved in this NCS as: $\hat{n}_N = (0, s(\varepsilon_N), c(\varepsilon_N))$.

Given ε_N and Eq. (16) for $\rho_C(\psi_C)$, our goal is to obtain a general formula for $\rho_N(\psi_N)$, and then specialize to the cases $\varepsilon_N = \varepsilon_D$ and $\varepsilon_N = \varepsilon_H$. Exact results analogous to (16) are presently not available, but it will be seen that accurate formulas linear in α can be obtained. The linearizations are possible because it will be seen that both ε_D and ε_H are of order α. Thus, the following approximate expression for ε_D (accurate to $2\text{x}10^{-6}$ deg) can be derived using the results of Heffron and Watson[9]:

$$\varepsilon_D \approx \left[\frac{\alpha}{2+\alpha}\right]\left[\frac{(R-R_D)\,s(2\lambda)}{R-\left(\frac{\alpha}{2+\alpha}\right)(R-2R_D)\,c(2\lambda)}\right] \qquad (24)$$

where

$$R_D \approx R - \frac{a}{\sqrt{1+\alpha\, s^2(\lambda)}}\ . \qquad (25)$$

Linearizing in α yields:

$$\varepsilon_D \approx \frac{\alpha}{2}\, s(2\lambda)\, s(\rho_0)\ . \qquad (26)$$

A similar expression can be derived[2,3] for the horizon bisector nadir $\hat{n}_H$ by equalizing the values of ρ in the local North and South directions. Starting from the Eq. (16), we can show that (see Appendix A)

$$\varepsilon_H \approx \frac{\alpha}{2}\, s(2\lambda)\, s^2(\rho_0)\,, \qquad (27)$$

and that, to order α, ρ_H will be equal for *any* pair of diametrically opposite horizon points. (This is particularly useful in analyzing the Barnes static Earth sensor assembly[3-6] where the sensor axes do not coincide with the $\hat{x}_H$ and $\hat{y}_H$ axes.)

Equations (19), (26), and (27) show that ε_D and ε_H are generated from ε_{ell} by successive applications of the factor $s(\rho_0)$ which is nearly unity for low-Earth orbiting spacecraft. As a practical example, consider TRMM for which the maximum value of λ is 35 deg, and R is about 350 km. Then $s(\rho_0)$ = 0.9510, and $s(2\lambda)\big|_{\max}$ = 0.9397, so that the maximum values of the tilt angles ε_{ell}, ε_D, and ε_H are respectively 0.1814 deg, 0.1725 deg, and 0.1641 deg. Thus, nominal pointing in either the geodetic or horizon bisector frames implies near-normal viewing of the horizon ellipse. We also conclude that $\hat{n}_H$ is very close to $\hat{n}_D$; for TRMM the difference is less than 0.01 deg, and corresponds to a surface arc length of only about 0.05 km.

A Linearized Formula for the Earth Angular Radius, $\rho_N(\psi_N)$

The angular radius of the nearly spherical Earth can be obtained from the following linearization of Eq. (16):

$$t(\rho_C) - t(\rho_0) \approx -\frac{\alpha}{2}\, t(\rho_0)\left[\, s(\lambda)\, t(\rho_0) + c(\lambda)\, s(\psi_C)\right]^2 . \qquad (28)$$

Thus,

$$\rho_C(\psi_C) - \rho_0 \approx -\frac{\alpha}{4}\, s(2\rho_0)\left[s(\lambda)\, t(\rho_0) + c(\lambda)\, s(\psi_C)\right]^2 . \qquad (29)$$

A similar expression for ρ_N can be derived using spherical geometry[10]. We obtain the complementary relations

$$c(\rho_N) = c(\rho_C)\, c(\varepsilon_N) - s(\rho_C)\, s(\varepsilon_N)\, s(\psi_C)\,, \qquad (30)$$

and

$$c(\rho_C) = c(\rho_N)\, c(\varepsilon_N) + s(\rho_N)\, s(\varepsilon_N)\, s(\psi_N)\,. \qquad (31)$$

These can be linearized in ε_N to yield

$$\rho_N \approx \rho_C + \varepsilon_N\ s(\psi_C)\,, \qquad (32)$$

and

$$\rho_C \approx \rho_N - \varepsilon_N\ s(\psi_N)\,. \qquad (33)$$

Using Eq. (28) and ignoring the difference between ψ_N and ψ_C (which is of order ε_N as shown in Appendix B) yields

$$\rho_N(\psi_N) \approx \rho_0 - \frac{\alpha}{4}\, s(2\rho_0)\left[s(\lambda)\, t(\rho_0) + c(\lambda)\, s(\psi_N)\right]^2 + \varepsilon_N\ s(\psi_N)\ . \qquad (34)$$

Defining ρ^* and $\Delta\rho(\psi_N)$ via

$$\rho^* \equiv \rho_0 - \frac{1}{2}\alpha\, s(\rho_0)\, t(\rho_0)\, s^2(\lambda) \qquad (35)$$

and

$$\Delta\rho(\psi_N) \equiv -\frac{1}{4}\alpha\, s(2\rho_0)\, c^2(\lambda)\, s^2(\psi_N), \qquad (36)$$

and using the formula for ε_H in (27), (34) may be written as

$$\rho_N(\psi_N) \approx \rho^* + \Delta\rho(\psi_N) + (\varepsilon_N - \varepsilon_H)\, s(\psi_N). \quad (37)$$

We expect that ρ^* will deviate significantly in from ρ_0 due to $t(\rho_0)$ which appears in Eq. (35); by the same token, $\Delta\rho(\psi_N)$ will contribute much less since $s(2\rho_0)$ may be written as $2s(\rho_0)/\, t(\rho_0)$ in Eq. (36) with $s(\rho_0) \approx 1$.

Let us now consider the horizon bisector coordinate system. By definition, the term proportional to $s(\psi_H)$ in (37) vanishes. The remaining ψ_H -dependence in (37) arises only via $s^2(\psi_H)$ in $\Delta\rho$, thus showing that $\rho_H(\psi_H) = \rho_H(\psi_H + \pi)$ for arbitrary ψ_H. This shows the (approximate) equality of the angular radii for any two diametrically opposite horizon points, thus validating the term "horizon bisector".

Let us now use (37) to evaluate the ψ_H -dependence of $\Delta\rho(\psi_H)$, which is

$$\frac{\partial\rho_H}{\partial\psi_H} \approx -\frac{\alpha}{4}\, s(2\rho_0)\, c^2(\lambda)\, s(2\psi_H) \quad . \qquad (38)$$

For TRMM, ρ_0 = 1.25630 = 71.9807 deg. Thus, the maximum of $\left|\frac{\partial\rho_H}{\partial\psi_H}\right|$ for λ = 0 deg and 35 deg are only 0.000991277 and 0.000665157 respectively. More explicitly, the numerical values of ρ_H for ψ_H = 0 deg and 90 deg are listed below for λ = 0 deg and 35 deg.

ρ_H (λ = 0 deg, ψ_H = 0 deg) ≈ 71.9807 deg

ρ_H (λ = 0 deg, ψ_H = 90 deg) ≈ 71.9807 deg
- 0.0567960 deg

ρ_H (λ = 35 deg, ψ_H = 0 deg) ≈ 71.8041 deg

ρ_H (λ = 35 deg, ψ_H = 90 deg) ≈ 71.8041 deg
- 0.038111 deg

Thus ρ_H varies over one quadrant by less than 0.06 deg for TRMM. In view of the practically insignificant differences in the numerical values of ε_D and ε_H in Eqs. (26) and (27), and the relatively small contribution of $\Delta\rho(\psi_N)$, we may further approximate Eq. (37) by

$$\rho_H(\psi_H) \approx \rho_D(\psi_D) \approx \rho^* \quad . \qquad (39)$$

Note that ρ^* is not a true constant since it is a function of the spacecraft position via R and λ. Nevertheless it is independent of the attitude (the "yaw" angle, ψ_D , for Earth pointing spacecraft). This formula can be of use in quick calculations or when the accuracy requirements are modest.

Conclusions

We have derived exact expressions for the properties of the horizon ellipse including the angle ε_{ell} between its normal and the geocentric nadir, and an exact expression relating the angular radius, ρ_C, of the horizon from the geocentric nadir to the azimuthal angle, ψ_C, about this nadir. This expression for ρ_C agrees with earlier work[1].

The introduction of a generalized Nadir Coordinate System where a new nadir vector is generated from the geocentric nadir vector by a rotation ε_N about the local West was useful in

- deriving further exact properties such as the offset of the center of the ellipse when $\varepsilon_N = \varepsilon_{ell}$
- introducing coordinate systems from the point of view of an observer
- providing a unified treatment of the angular radius, ρ_N, of the horizon as a function of the azimuthal angle, ψ_N

Formulas linearized in α were derived for the geodetic and horizon bisector tilt angles ε_D and ε_H respectively, showing that they differ from ε_{ell} through successive factors of $\sin(\rho_0)$, where ρ_0 is the angular radius of the horizon contour in the spherical Earth approximation. Linearized expressions were also derived for $\rho_D(\psi_D)$ and $\rho_H(\psi_H)$ and showed that the tilt angle ε_H generates the desired horizon bisection effect.

Numerical application of the various formulas to the TRMM spacecraft (which uses static horizon sensors) as a typical example revealed the following.

- ε_{ell}, ε_D, and ε_H differ by less than 0.02 deg, that is, the geodetic and horizon bisector nadir vectors, $\hat{n}_D$ and $\hat{n}_H$, are nearly normal to the horizon ellipse
- $\hat{n}_H$ is a good approximation to $\hat{n}_D$ (to within 0.01 deg)
- ρ_H varies by less than 0.06 deg as the azimuthal angle ψ_H varies along the ellipse.
- The oblate Earth presents to the spacecraft an Earth disk which can be well-approximated by

a circle whose center is on $\hat{n}_D$ and whose radius, ρ^*, depends on the spacecraft position.

Appendix A - The Horizon Bisector Frame

Let $\vec{h}_+$ and $\vec{h}_-$ be the North and South horizon points, with the azimuth angle ψ_C equal to $+\pi/2$ and $-\pi/2$, respectively. Note that the azimuth angle ψ_N of these two horizon points also takes exactly the same values $+\pi/2$ and $-\pi/2$ in any NCS, and therefore it is immaterial as to which NCS is used to evaluate $\vec{h}_+$ and $\vec{h}_-$. Another important point is that both $\vec{h}_+$ and $\vec{h}_-$ are perpendicular to $\hat{x}_C$ and therefore their NCS angular radii ρ_N are related to their geocentric radii $\rho_C = \rho_\pm$ via the simple relation:

$$\rho_N\left(\psi_N \pm \frac{\pi}{2}\right) = \rho_\pm \pm \varepsilon_N \tag{A1}$$

which implies that

$$\varepsilon_H = (\rho_- - \rho_+)/2\,. \tag{A2}$$

Evaluating Eq. (16) at $\psi_C = \pm\pi/2$ we get

$$cot(\rho_\pm) = (F_2 \pm \Delta F_2)/F_1\,, \tag{A3}$$

where

$$F_1 \equiv s(\rho_0)\,\left(1+\alpha\, s^2(\lambda)\right), \tag{A4}$$

$$F_2 \equiv \sqrt{\left(c^2(\rho_0)+\alpha\, s^2(\lambda)\right)(1+\alpha)}\,, \tag{A5}$$

and

$$\Delta F_2 = \alpha\, s(\rho_0)\, s(\lambda)\, c(\lambda)\ . \tag{A6}$$

Knowing cot(ρ_+) and cot(ρ_-) from Eq. (A3), it is easy to show that

$$\tan(\rho_- - \rho_+) = \frac{2F_1\,\Delta F_2}{F_1^{\,2} + F_2^{\,2} - \Delta F_2^{\,2}}\,. \tag{A7}$$

Explicit evaluation of Eq. (A7) using the definitions in Eqs. (A4)-(A6), and the identity

$$\begin{aligned} 1+\alpha+\alpha\, s^2(\lambda)\, c^2(\lambda) \\ \equiv \left(1+\alpha\, s^2(\lambda)\right)\left(1+\alpha\, c^2(\lambda)\right) \end{aligned} \tag{A8}$$

yields the simple result

$$t(2\varepsilon_H) = \frac{\alpha\, s(2\lambda) s^2(\rho_0)}{1+\alpha-\alpha\, s^2(\rho_0)\, c(2\lambda)}\ . \tag{A9}$$

Linearization of Eq. (A9) in α and ε_H immediately yields Eq. (27).

Appendix B – The Azimuth Angle ψ_N Within the Nearly-Spherical Approximation

An explicit formula relating ψ_N to ψ_C can be obtained by summing up Eqs. (30) and (31), yielding

$$s(\rho_N)\ s(\psi_N) - s(\rho_C)\, s(\psi_C) = t\left(\frac{\varepsilon_N}{2}\right)\left[c(\rho_C)+c(\rho_N)\right] \tag{B1}$$

By linearizing the left side of this relation with respect to ρ_N -ρ_C and making use of Eq. (31) one finds

$$s(\psi_N) \approx s(\psi_C) + \varepsilon_N\, c^2(\psi_C)\, cot(\rho_C)\,. \tag{B2}$$

Note that the North and South horizon points $\psi_N = \pm\pi/2$ must lie in the $\hat{y}_N - \hat{z}_N$ plane and therefore, by definition, they are the same for any NCS. (Contrast this with the East and West horizon points which vary slightly for different NCSs). In fact, according to Eq. (B2), $\psi_N = \psi_C$ for $\psi_C = \pm\pi/2$, as expected.

References

[1]Liu, K.; "Earth Oblateness Modeling", in *Spacecraft Attitude Determination and Control*, Ed: J. R. Wertz, D. Reidel Publishing Co., Dordrecht, Holland, 1978, pp. 98-106

[2]Flately, T. W.; "TRMM Yaw", Technical Memorandum from 712.3/TRMM ACS lead analyst, D. McGlew, to Distribution, November 16, 1992.

[3]Challa, M.; "Advanced Attitude Determination Task Attitude Determination Using Static Earth Sensors: Models and Algorithms", Technical Memorandum No. 553-FDD-94/030R0UD0, prepared for NASA-Goddard Space Flight Center, August 1994

[4]Keat, J., Challa, M., Tracewell, D., and Galal, K.; "Earth Horizon Modeling and Application to Static Earth Sensors on TRMM Spacecraft", *Proceedings of the Flight Mechanics and Estimation Theory Symposium*, NASA Conference Publication No. 3299, Goddard Space Flight Center, Greenbelt, MD, May 1995

[5]Natanson, G.; "New Algorithms for the Simulation, Processing, and Calibration of Earth Sensor Penetration Angles", Technical Memorandum No. 27434-12, prepared for NASA-Goddard Space Flight Center, December 1996

[6]Natanson, G.; "Ground-Support Algorithms for Simulation, Processing, and Calibration of Barnes Static Earth Sensor Measurements: Application to the Tropical Rainfall Measuring Mission Laboratory ", *Proceedings of the Flight Mechanics Symposium*, NASA Conference Publication No. 3345, Goddard Space Flight Center, Greenbelt, MD, May 1997

[7]Challa, M.; "New Results on the Shape of the Earth Disk as Seen by a Spacecraft ", technical memorandum No. CSC-86-910-14, prepared for NASA-Goddard Space Flight Center, September 1998

[8]The TRMM home page on the web is at:
http://fpd-b8-0001.gsfc.nasa.gov/490/more/trmmhp.htm

[9]Heffron, W. G. and Watson, S., B.; "Relationships Between Geographic and Inertial Coordinates", Journal of Spacecraft and Rockets, vol. 4, pp. 531-532, April 1967

[10]Tandon, G. K..; in "*Spacecraft Attitude Determination and Control*", Ed: J. R. Wertz, D. Reidel Publishing Co., Dordrecht, Holland, 1978, pp. 760-766. In the notation of this reference, ρ_N is the angle between the points ($\phi = -\psi_C$, $\theta = \rho_C$) and ($\phi_0 = \pi/2$, $\theta_0 = \varepsilon_N$).